

Journal Pre-proofs

An investigation on residual stress and fatigue life assessment of T-shape welded joints

Farzaneh Samadi, Jeetendra Mourya, Greg Wheatley, Mohammed Nizam Khan, Reza Masoudi Nejad, Ricardo Branco, Wojciech Macek

PII: S1350-6307(22)00655-0
DOI: <https://doi.org/10.1016/j.engfailanal.2022.106685>
Reference: EFA 106685

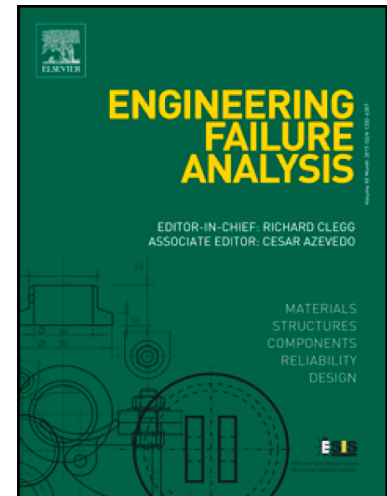
To appear in: *Engineering Failure Analysis*

Received Date: 6 July 2022
Revised Date: 22 July 2022
Accepted Date: 27 July 2022

Please cite this article as: Samadi, F., Mourya, J., Wheatley, G., Nizam Khan, M., Masoudi Nejad, R., Branco, R., Macek, W., An investigation on residual stress and fatigue life assessment of T-shape welded joints, *Engineering Failure Analysis* (2022), doi: <https://doi.org/10.1016/j.engfailanal.2022.106685>

This is a PDF file of an article that has undergone enhancements after acceptance, such as the addition of a cover page and metadata, and formatting for readability, but it is not yet the definitive version of record. This version will undergo additional copyediting, typesetting and review before it is published in its final form, but we are providing this version to give early visibility of the article. Please note that, during the production process, errors may be discovered which could affect the content, and all legal disclaimers that apply to the journal pertain.

© 2022 Published by Elsevier Ltd.



An investigation on residual stress and fatigue life assessment of T-shape welded joints

Journal Pre-proofs

wojciech macek*

¹Department of Materials, Faculty of Engineering, Semnan University, Semnan, Iran

²College of Science and Engineering, James Cook University, Townsville QLD 4811, Australia

³College of Engineering, Science & Technology, Fiji National University, Derrick Campus, Samabula, Fiji

⁴School of Mechanical and Electrical Engineering, University of Electronic Science and Technology of China, Chengdu, 611731, China

⁵University of Coimbra, CEMMPRE, Department of Mechanical Engineering, Coimbra, Portugal

⁶Gdansk University of Technology, Faculty of Mechanical Engineering and Ship Technology, 11/12 Gabriela Narutowicza, Gdańsk 80-233,

Poland

Abstract

This paper aims to quantitatively evaluate the residual stress and fatigue life of T-type welded joints with a multi-pass weld in different direction. The main research objectives of the experimental test were to test the residual stress by changing direction along with multiple welding passes and determine the fatigue life of the welded joints. The result shows that compressive residual stress increases in the sample gradually from single-pass weld to double and triple-pass weld. Moreover, the fatigue life of the specimen also gradually improves with an increasing number of welding passes. Performing multi-pass welding in different directions affects the material's residual stress and fatigue life, which is an essential factor to consider for assuring the strength of the welded joint.

Keywords: Residual stress; Fatigue life; Multi-pass weld; Bisalloy 80; Strain gauge.

1. Introduction

One of the important factors in the design of structures is the design of joints and its strength [1-3]. Welding is a type of processing used to combine different materials to create a joint [4-6]. The need to predict the mechanical strength of engineering components leads to analyzing the stress distribution within the joint itself [7-9]. The joints between two or more separate sections of material are formed during welding. Welding of metallurgical materials is majorly used in building structures, mining equipment's, bridges, ships, and defence services [10]. The main advantages of using these welded structures involve excellent joint efficiency, less

* Corresponding author.

E-mail addresses: frzn.samadi@gmail.com (F. Samadi), jeetendra.mourya@my.jcu.edu.au (J. Mourya), greg.wheatley@jcu.edu.au (G. Wheatley), mohammed.k@fnu.ac.fj (M.N. Khan), masoudinejad@uestc.edu.cn (R. Masoudi Nejad), ricardo.branco@dem.uc.pt (R. Branco), wojciech.macek@pg.edu.pl (W. Macek).



fabrication charge and high air and water tightness [11]. Tensile residual stress exists on the welded joints due to shrinking when cold [12-14]. Consideration of this residual stress is vital during structural designing. The main disadvantage of this residual stress is that it can introduce

when high external stress above a specific limit is applied. Nevertheless, due to local heat produced by welding practice and quick cooling, residual stress can introduce near the weld joint. This high residual stress can induce cracks, brittle fractures, and fatigue at the welded region. Moreover, it also decreases the buckling strength of the structure plates [19]. **Therefore, residual stress from the welding process must be minimized to prevent premature structure failure.**

Residual stresses impact the performance of structural materials in different ways and are usually present at the joint surface or sub-surface of the welded region. The common effects are fatigue, stress corrosion, failures, distortions, structural stability [20]. Depending upon whether the focus is tensile or compressive, residual stress may be detrimental or beneficial. Residual stresses of the tensile may be too high to deform or break the components. In addition, tensile stresses are needed to produce fatigue and stress corrosion cracking [21]. As residual stresses are combined with quantitative applied stress, residual tensile stresses on the surface combined with tensile stress can reduce component reliability [22]. Indeed, occasionally residual tensile stress triggers stress cracking. Evaluating residual stress in the welded region provided insights into the internal stress acting on the structure. However, several factors, including change in mechanical and thermal behavior due to high heating temperature in the welding process, makes it difficult to accurately predict the residual stresses [23-25]. Therefore, estimating the total stress, including external and internal pressure such as residual stress, is essential while structural designing. In structures, welded joints are assumed to be the weakest point because of stress concentrations and the low yield strength of the joint material. The fatigue may result in a welded joint subject to cyclic loading [26]. Fatigue occurs as well as strains in the material from this cyclic loading. Cracks that decrease the fatigue life of a jointed assembly begin, spread and expand over the entire lifetime of a welded assembly, causing the assembly to fail even though these cyclic stresses are smaller and smaller than the base material, and the welded material generating stress [27, 28]. Hence, the welded joint fatigue was minimized failures by integrating design considerations into the development process. There are different ways to minimize the residual stress in the welded structure. Pre-heating, hammering, vibration stress, weld sequence and arc welding are common approaches used to reduce this stress in the joint region [29]. **Gas arc welding is the most popular method,**



encompassing MIG (Metal Inert Gas) welding, TIG (Tungsten Inert Gas) welding, stick welding and flux-cored welding. Arc welding processes are the most used of the welding methods, and most of the remaining stresses and distortions produced to date have been on

In most cases, the necessity arises to design and analyze components with complex geometries and properties under irregular loads, then the use of existing classical methods causes finding highly complex governing equations with varied boundary and initial conditions which make it impossible to solve these equations analytically, and therefore, numerical methods should be utilized to deal with the conundrum [30-32]. Numerical and analytical methods are used to determine the fatigue life of engineering structures. Most numerical methods are verified by experimental and analytical methods [33-35]. The temperature distribution in the weld is uniform and varies as the welding advances because of the heating locally of a weld [36, 37]. In the weld metal regions and base metal close the weld, the dynamic thermal cycle creates non-elastic strains. These non-elastic strains create residual stress as the weld cools to the very first temperature. Another study determined the residual stress effects on the fatigue life of the welded joint [38]. The study showed that fatigue life decreases with a high rate of fatigue crack when increasing tensile residual stress. MIG welding is an arc welding process in which a wire electrode is combined through a welding gun between joints to combine two base materials. Simultaneously a shielding gas flows in the welding gun for protecting the weld pool from contamination. This type of welding is quick and gives a long arc time even if the electrodes are not ultimately charged. Effect of Multi-pass welding on residual stress and fatigue life of the welded material Various factors like heat and multi-pass welding, including sequence of weld pass and direction, could alter the magnitude of residual stresses [39]. The past study proved that the peak values of longitudinal and transversal residual stress decreased by 17% when welding in inverse direction compared to the results obtained with welding in the same order [40]. These studies concluded that directional change in welding passes might affect the magnitude of residual stresses in the welded regions. Liu et al. concluded that if multiple weld passes were performed instead of a single pass, and when doing the multi-pass weld reduced the weld's depth, the residual stresses can be changed the fatigue life of the structure [41]. Massive steel constructions feature many welded connections, some of which are single layer welded and multi-pass welded, depending on the strength [42]. Significant residual stresses, which often surpass the material yield stress, are common in welded systems [23]. Knowing the value of residual stress and fatigue life of various weld pass types before constructing the structure would aid the designing engineers in considering overall stresses and building the



structure accordingly [38]. This was help eliminate inaccuracies in a structure's stress computation, resulting in increased accuracy in all areas. These studies highlight that welding sequences with different directions of weld passes can significantly influence the magnitude of

High residual stress in the welded joints may introduce brittle fatigue or fractures. High tensile residual stress significantly affects the fatigue life of the welded structures, and compressive residual stress has a favorable impact on fatigue life [43-45]. This combination may endorse failure by fatigue. Several stress-reducing welding processes, including multi-pass welding, have been adopted to predict fatigue life and distortion in the material to obtain accurate residual stress distributions [46-48]. The convenient and efficient method is to select a proper welding sequence that effectively reduces residual stress because the varying degree of residual stress on welded structures can cause post-weld manufacturing consequences. Therefore, it is essential to determine the effect of welding sequences on the specimen's uneven residual stresses and fatigue life. The present study was tested how multi-pass welding in different directions can affect the structural material's residual stress and fatigue life. The main research objectives of the experimental test were to calculate the residual stress by changing welding direction with different welding passes and determine the fatigue life of the welded specimen. The experimental test was performed multi-pass welding with different directions to determine residual stress changes and test fatigue life in the multi-pass welded joint. In the experimental tests, the MIG welding type was used to evaluate the residual stress and its effect on the fatigue life of welded joined structure.

2. Materials and methods

The analysis was determined whether the residual stresses differed between the weld pass types and whether that affected fatigue. Bisalloy 80 steel was utilized for the unusually high application of MIG to ensure that fatigue failure happens at the welding with all wires utilized with a diameter of 0.9 mm. There was no cooling time between the first and the consecutive overlaying weld during the welding process. For testing residual stress and fatigue strength, 12 samples were prepared for all passes (single, double and triple) with four samples in each pass. Out of the four samples, one was used for residual stress testing, and the remaining three were used for fatigue life testing. Fatigue crack growth tests were performed using the Instron machine, for which three samples of single weld pass were used, three of double weld pass, and three of triple weld pass. Among all 12 samples made, three samples were made for residual stress testing and 9 for fatigue crack growth testing. A single pass weld on both sides of the T-

intersection point for the first specimen was performed. The direction of the weld is shown in Figure 1. The width of the weld was 12 mm for this specimen.

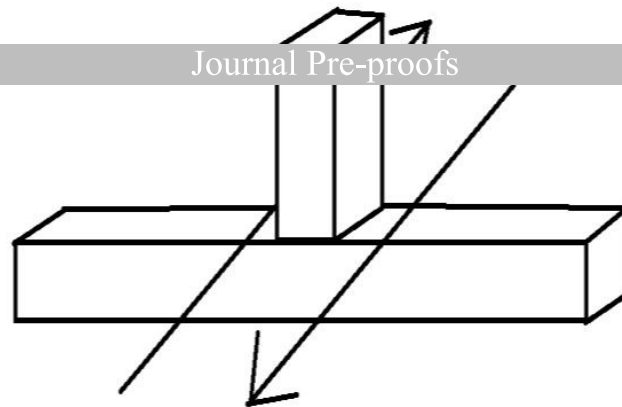


Figure 1. The direction of single weld pass.

For the second specimen, a double pass weld was performed. The first pass of weld on the specimen was followed by specimen 1 but only 6 mm of weld this time. For the second overlapping weld, the direction of the weld pass was opposite to the first weld pass on both sides. The width of the second weld pass was 6 mm. The total weld width was 12 mm. For the third specimen, a triple-pass weld was performed. The first and second weld pass on the specimen was followed by specimen 2. For the third overlapping weld, the direction of the pass was opposite to the second weld, as shown in Figure 2. The width of the weld passes was used this time was 4 mm each on both sides, and after the third welding, overlapping of 4 mm was done, thus contributing to the overall 12 mm width of the weld.

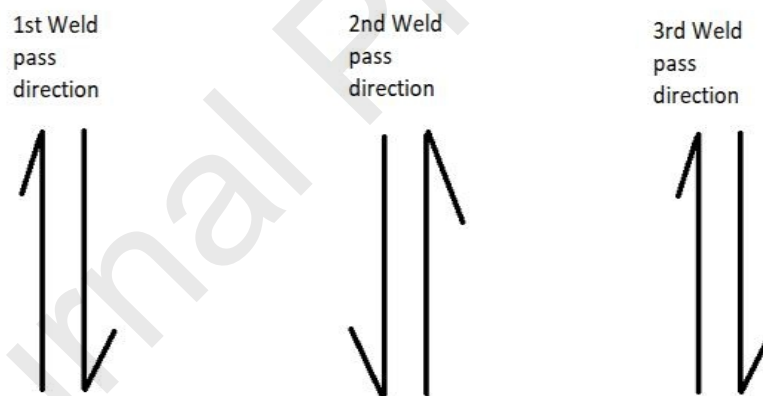


Figure 2. Directions of multi-pass weld in sequence.

The residual stresses of the samples were determined by strain gauges (Bestech FLAB-5-11-3LJC-F gauges of $2.1 \pm 1\%$ gauges). These strain gauges were positioned at the base of the bottom plate just below the weld position. Figure 3 shows that the strain gauges were secured with Eythl 2-cyanoacrylate on both sides of the T-joint. A hydrocarbon solvent was used in the

region where the strain gauges were positioned for all the residues of flux and strains to be removed.



Figure 3. Strain gauges below the base plate parallel to the weld joints.

The experimental approach was confined to quantifying the residual stress in the heat and welding area. An increase of 0.5 mm was machined into the base plate from the top of the weld through a 50 mm tool-fitted computer numerical control (CNC) machine. During the procedure, bolts were employed to limit the specimen's movement. The bolted joints fastened rubber cushions to eliminate harmonic spikes in the strain data. A Vernier digital calliper was employed between each framing interaction for accurate cutting measures to measure the specimen height.

The fatigue life of the specimens was determined by performing high cycle fatigue life testing on the Instron machine (Figure 4). The amplitude of the testing was 12 mm with a 5 Hz frequency same for all the specimens. The specimens were tested till they got to the complete failure point.



Figure 4. Experimental test setup.

3. Results and discussion

3.1. Residual stress

Figure 5 shows the peak stress values, and the depth of the milling from the starting point of weld to it reaches 5 mm in the base plate. Figure 5 shows milling depth on X-axis. Milling of the single weld pass sample started with a milling depth of 0.5 mm/mill. This specimen was 32 mm in height. First, the 12 mm weld above the base plate was milled, then milled 5 mm below the base plate top surface. A total of 34 milling operations were done on the T-specimen. The maximum stress in this sample was observed at 3 mm below the top surface of the base plate, and the value of the obtained stress is 79202.70 Pa.

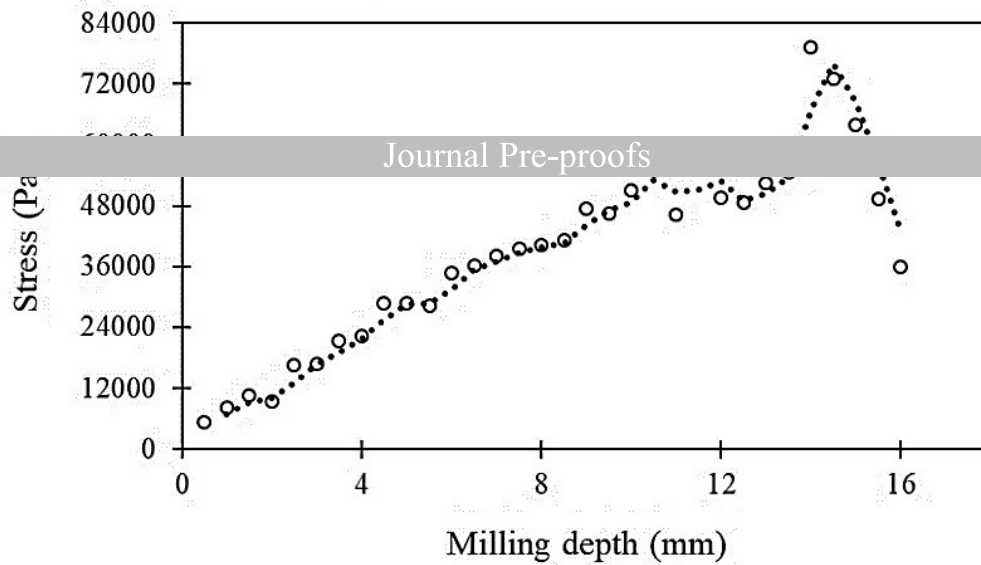


Figure 5. Single-pass peak stress vs. milling depth.

After milling 10.5 mm of the sample from the top, the height was checked using a digital vernier calliper. The expected height was 21.5 mm, but it was measured at 21.44 mm. This difference in the height of 0.06 mm can be due to compression in the base plate of the sample. The same phenomenon was observed again when the sample's height was measured after milling 15 mm, and this time, the expected height was 17 mm, but with a difference of 0.12 mm, it was measured 16.88 mm. A crack line was observed at a depth of 9 mm from the top surface on both sides of the t-shape specimen, as shown in Figure 6. It means that the welding did not penetrate the metal plate properly in this specimen. This fusion reduces the compressive residual stress in this sample as the weld is not strong at the bottom of the sample.

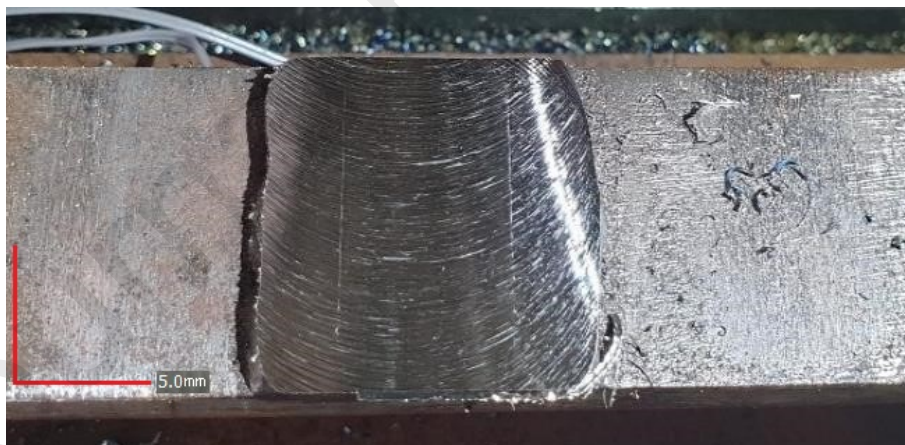


Figure 6. Crack observed in single weld specimen.

Figure 7 exhibits the depth of the milling along the x-axis and the value of peak stress along the y-axis. This specimen was 32 mm in height from the bottom of the base plate to the top

surface. It took 34 times a mill of 0.5 mm to complete the milling of 17 mm of the specimen from the top. As shown in the below graph, the maximum stress value is 16 mm from the top of the base plate, and the stress value is 85986.56 Pa.

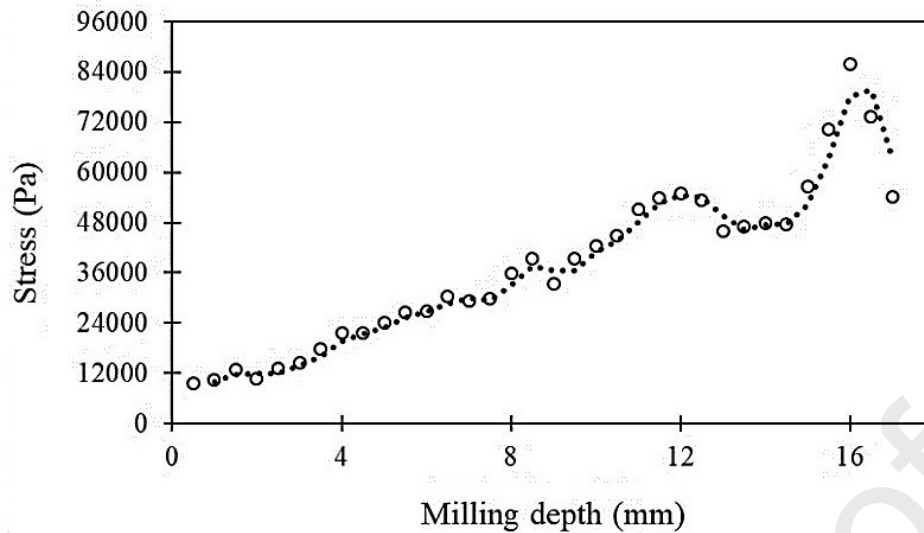


Figure 7. Double pass peak stress vs. milling depth.

The height difference was also observed in this sample at 10.5 mm and 15 mm, and it was 0.05 and 0.1 mm, respectively. After milling 11 mm, a fine weld crack was observed; the crack was not apparent as the single-pass weld sample had **but could explain that weld did penetrate through the surface of the sample at this point.** Figure 8 shows the peak stress values of a triple weld pass specimen milled 34 times at 0.5 mm mill per reading. In this specimen, **the height of the whole specimen was 32 mm (i.e., 12 mm weld and 20 mm base plate).** The maximum stress value obtained for this sample is 77491.670 Pa at a depth of 15 mm. A height difference was also seen when measured after 10.5 mm and 15 mm milling, and the difference was 0.03 mm and 0.13 mm, respectively.

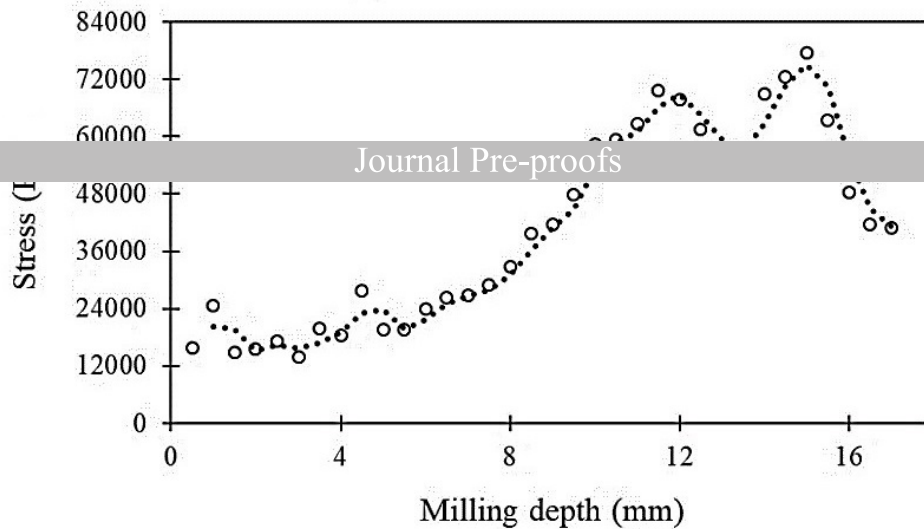


Figure 8. Triple pass peak stress vs. milling depth.

Milling at a depth of 10 mm depth, small pits were observed. Further, no such defects were observed on the sample surface. These pits can result from unremoved residual flux during overlapping the weld. No fusion crack line was seen in this sample, which implies that the welding was correctly done, resulting in high compressive residual stress in the weld. **Figure 9 shows cavity observed in triple weld specimen.**



Figure 9. Cavity observed in triple weld specimen.

Residual stress is calculated and plotted **using the residual stress formula and the observed strain values of the specimens.** Only the first 1 mm affects the sample's fatigue life; therefore, the residual stress value of the first 1 mm mill is considered. As shown in Figure 10, the compressive residual stress values of single weld pass, double weld pass, and triple weld pass in the first 1 mm of milling are 8268.1 Pa, 10328.782 Pa, and 24625.731 Pa, respectively.

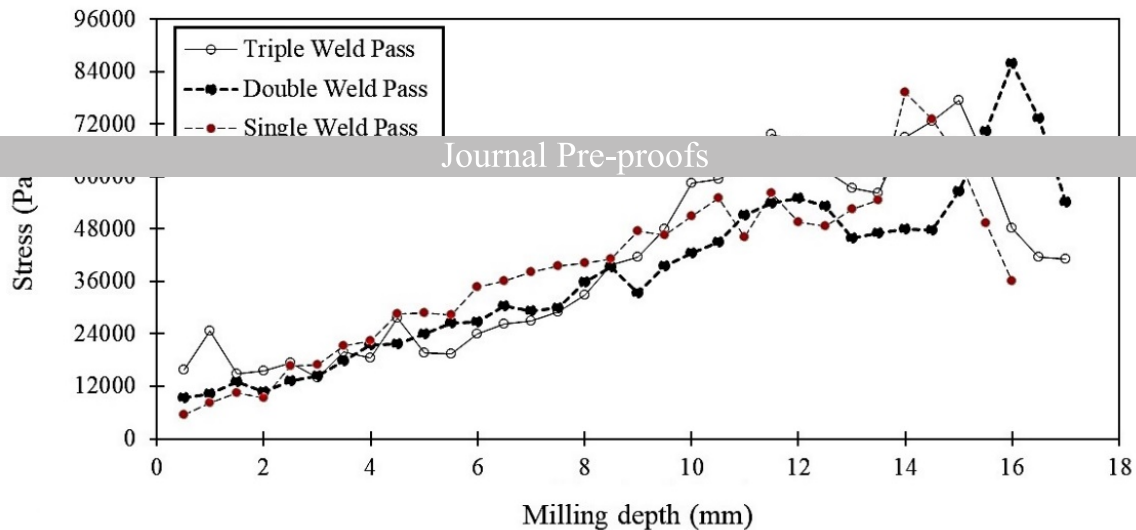


Figure 10. Residual stress vs. milling depth.

In the welding process, the welded area of the specimen undergoes tension. During milling of the specimens, layer the weld in milled and remove, which causes the specimen to go under compression and achieve stability. This phenomenon explains a height difference in all the three samples when measured after milling 10.5 mm and 15 mm from the top. This mechanism is recorded using datalogger CR1000x and strain gauges. The strain gauges are placed below the base plate parallel to the weld joints, as shown in Figure 1. An accurate change in strain is calculated. The compressive residual stress values of single weld pass, double weld pass, and triple weld pass in the first 1 mm of milling are 8268.1 Pa, 10328.782 Pa, and 24625.731 Pa, respectively. It was also observed that due to the unpolished weld surface in the multi-pass weld, there is leftover residual material generated on the surface, which affected the strength of the weld in double and triple pass weld. A multi-pass weld needs to polish the first below layer before putting the weld above it to avoid discontinuity and defects in the weld. When comparing the residual stress values obtained, it can be seen that the compressive residual stress increases when increasing the weld pass. The highest compressive residual stress is for the triple-pass weld sample, next is for the double pass weld sample, and then the single-pass, which has the lowest residual stress. Hence, it can be concluded that multi-pass weld with changing directions has affected the residual stress in the specimen.

3.2. Fatigue crack growth test

An Instron machine was used to test the fatigue crack growth of the specimens. Method setup on the Instron machine was based on amplitude testing. The test performed 12 mm amplitude (means the specimen is stretched 6 mm in a positive direction and 6 mm in a negative direction

from the start point.). The frequency for all the testing is 5 Hz (cycles/sec). In experimental test, the specimen undergoes harmonic motion. Thus, the data appears in the form of a sine graph.



Figure 11. Positioning of sample in Instron machine.

Sample 1 went through 2000 cycles with 8 mm amplitude at 5 Hz, then 2000 cycles at 12 mm. Although the amplitudes were different, the specimen load was constant. All the specimens were tested at the same amplitude and frequency. From Figure 12, it can be seen that the average no of cycles a single weld pass specimen can withstand is between 5200-5600 cycles at 12 amplitude of movement and 5 Hz of frequency. Bisalloy 80 steel was utilised for the unusually high application of MIG to ensure that fatigue failure happens at the welding. Sample 1 completed 12700 cycles which were higher than the other two samples. The number of cycles done by sample 2 was 12000, closer to what sample 1 achieved. Sample 3 was observed and got a crack at 6500 cycles; this can be due to many different factors. One of the reasons, as discussed in the residual testing of double pass samples there were some unwanted materials left on the surface, which led to weakening the weld strength can be a cause. If an average value is taken, it can be seen that the double pass specimen has a fatigue life ranging between 11000 – 12000 cycles. Figure 13 shows crack in single weld, double weld, and triple weld sample 2. All the samples of this specimen showed a similar property and withstood a minimum of 23400 cycles. As shown in Figure 13-c, sample 2 experienced two cracks.

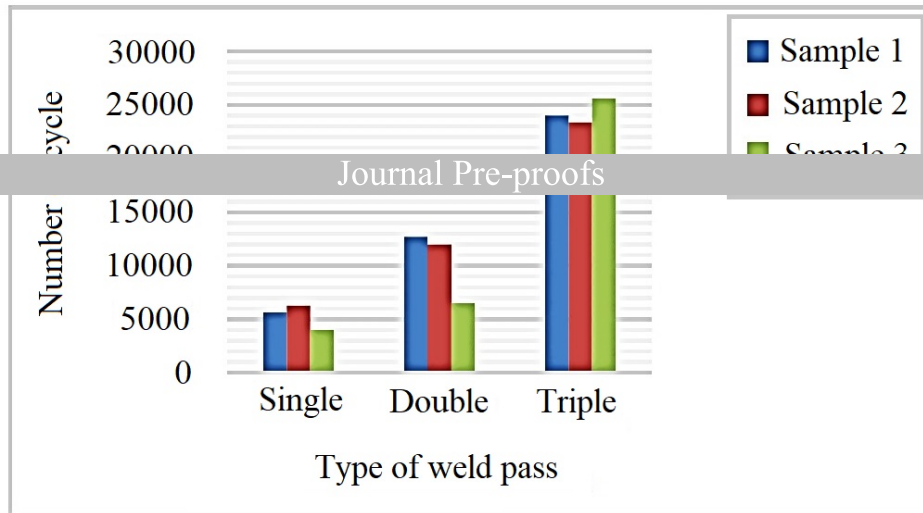
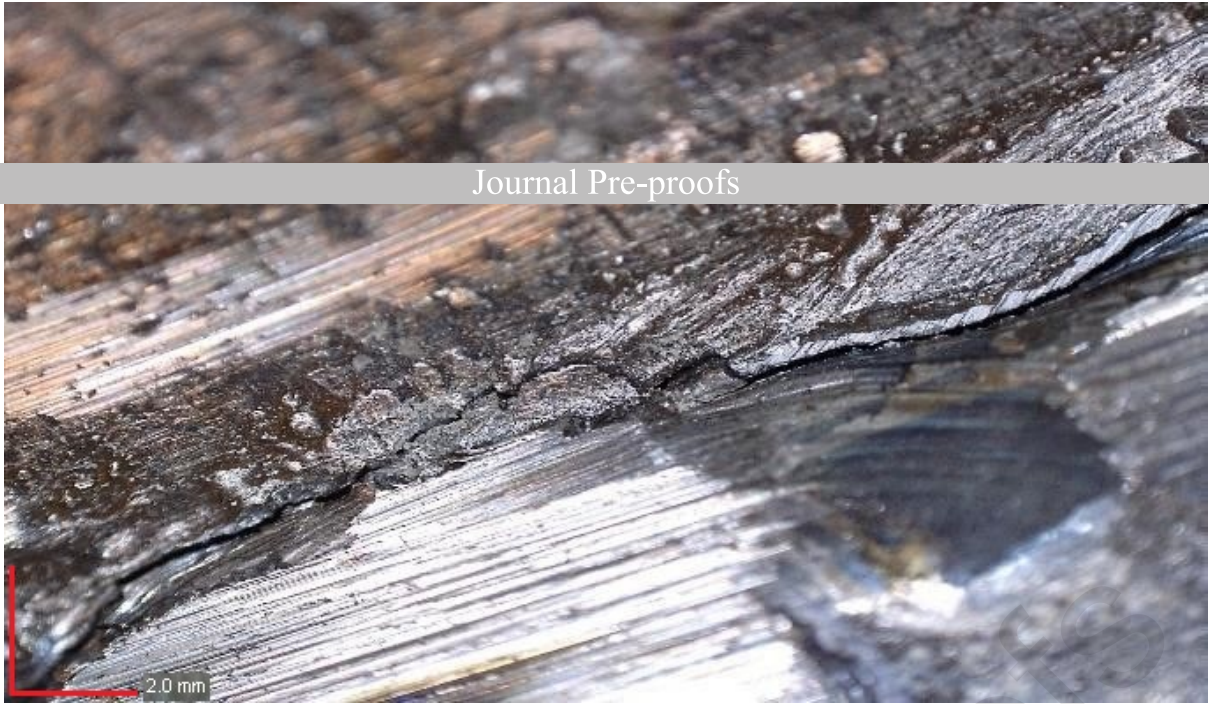


Figure 12. The number of cycles vs. weld pass.



(a)



(b)



(c)

Figure 13. Fatigue crack growth path in sample 2 for; a) single weld, b) double weld, and c) triple weld.

The above discussion concluded that the fatigue life of the specimens increases significantly with single, double, and triple weld pass. The double weld's fatigue life cycle is approximately twice that of the fatigue of a single weld pass. As discussed in the method section, the welding

experienced constant heat at a very high temperature. The contact area of the welded joint of the first weld pass covers more surface area than double or triple pass. This means that the welded layers exhibit a stronger bond at the joints due to consecutive continuous heating in the specimen, leading to higher fatigue life. Due to this phenomenon, the weld layers in sequence exhibit their adhesive strength with the metal surface.

4. Conclusions

Welding of structures causes prominent weak points in the structure. These weaknesses need to be factored in when calculating the strength capabilities. Reducing the stress concentration and weak points are key to designing a long lasting, high strength structure. This paper is presented the residual stresses and fatigue life prediction of multi-pass welded samples across different weld directions. In experimental test results, an increase in compressive residual stress was observed with an increase in weld pass. Moreover, the fatigue life of the sample gradually improves with an increasing number of welding passes. It is concluded that the triple-pass welded joint obtained enhanced fatigue strength with optimum compressive residual stress. This could be due to reheating at a high temperature during the multi-pass welding. The time taken to perform the second weld in the opposite direction of the first weld pass contributed to a slight rise in temperature. However, while performing the third weld pass (in the same direction as the first weld pass), the first welded region/layer becomes cool, resulting in higher compressive residual stress. This change in temperature and direction of the weld contributes to a more significant compressive residual stress and improved fatigue strength at the triple-pass welded joint. Therefore, multi-pass welding in different directions influences the change of residual stress and fatigue life. Future studies may include more experimental test of the residual and fatigue crack growth test with finite element method to guarantee the validity of the results and real-time implementation to promise structural integrity in various industrial applications.

References

[1] Ning, F., He, G., Sheng, C., He, H., Wang, J., Zhou, R., Ning, X. (2021). Yarn on yarn abrasion performance of high modulus polyethylene fiber improved by graphene/polyurethane

composites coating. *Journal of engineered fibers and fabrics*, 16. doi: 10.1177/1558925020983563

[2] Mousavi, A. A., Zhang, C., Masri, S. F., & Gholipour, G. (2021). Structural damage

Journal Pre-proofs

adaptive noise: a model steel truss bridge case study. *Structural health monitoring*, 84049609. doi: 10.1177/147592172111013535

[3] Hua Huang, M. A., Huang, M., Wei Zhang, M. A., Pospisil, S., & Wu, A. T. (2020). Experimental Investigation on Rehabilitation of Corroded RC Columns with BSP and HPFL under Combined Loadings. *Journal of Structural Engineering*, 146(8). doi: 10.1061/(ASCE)ST.1943-541X.0002725

[4] Liang, Z. M., Wang, G. Y., Sun, Z. B., Wang, D. L., WeiWang, L., MeiLiang, Y. (2022). Rapidly improved tensile strength of 6N01 Al alloy FSW joints by electropulsing and artificial aging treatment. *Materials Science and Engineering: A*. doi: 10.1016/j.msea.2022.143056.

[5] Zhong, Y., Xie, J., Chen, Y., Yin, L., He, P., Lu, W. (2022). Microstructure and mechanical properties of micro laser welding NiTiNb/Ti6Al4V dissimilar alloys lap joints with nickel interlayer. *Materials Letters*, 306. doi: 10.1016/j.matlet.2021.130896

[6] Guo, J., Gao, J., Xiao, C., Chen, L., & Qian, L. (2021). Mechanochemical reactions of GaN-Al₂O₃ interface at the nanoasperity contact: Roles of crystallographic polarity and ambient humidity. *Friction*. doi: 10.1007/s40544-021-0501-9

[7] Zhang, J., Wang, X., Zhou, L., Liu, G., Adroja, D. T., Da Silva, I., Jin, C. (2022). A Ferrotoroidic Candidate with Well-Separated Spin Chains. *Advanced materials (Weinheim)*, 34(12), e2106728. doi: 10.1002/adma.202106728

[8] Xu, H., He, T., Zhong, N., Zhao, B., & Liu, Z. (2022). Transient thermomechanical analysis of micro cylindrical asperity sliding contact of SnSbCu alloy. *Tribology international*, 167, 107362. doi: 10.1016/j.triboint.2021.107362

[9] Yang, G., Feng, X., Wang, W., OuYang, Q., & Liu, L. (2021). Effective interlaminar reinforcing and delamination monitoring of carbon fibrous composites using a novel nano-carbon woven grid. *Composites science and technology*, 213, 108959. doi: 10.1016/j.compscitech.2021.108959

[10] Sheng, C., He, G., Hu, Z., Chou, C., Shi, J., Li, J., Ning, F. (2021). Yarn on yarn abrasion failure mechanism of ultrahigh molecular weight polyethylene fiber. *Journal of engineered fibers and fabrics*, 16, 1925832385. doi: 10.1177/15589250211052766

[11] Asgarian, B., Mazaheri, P., & Gholami, H. Comparison of fatigue life assessment of tubular joints using different editions of API RP-2A standards. Proceedings of the 10th National Conference on Structures and Steel, 2019, Tehran, Iran.

Journal Pre-proofs

of periodic overload.” Engineering Failure Analysis, 115, 104624 (2020).

[13] Masoudi Nejad, R. “The effects of periodic overloads on fatigue crack growth in a pearlitic Grade 900A steel used in railway applications.” Engineering Failure Analysis, 115, 104687 (2020).

[14] Moradi, H., Beh Aein, R. and Youssef, G., 2021. Multi-objective design optimization of dental implant geometrical parameters. International Journal for Numerical Methods in Biomedical Engineering, 37(9), p.e3511.

[15] Wenchen Ma. (2021). “Behavior of Aged Reinforced Concrete Columns under High Sustained Concentric and Eccentric Loads,” Doctoral Thesis, University of Nevada, Las Vegas, Nevada, USA, 198 p.

[16] Behnam Niknam, Farhad Haji Aboutalebi, Wenchen Ma, Reza Masoudi Nejad. (2021). “Effect of variations internal pressure on cracking radiant coils distortion,” Structures, Vol 34, pages 4986-4998.

[17] Wanhai Xu, Yuhan Li, Wenchen Ma, Kai Liang, Yang Yu. (2020). “Effects of spacing ratio on the FIV fatigue damage characteristics of a pair of tandem flexible cylinders,” Applied Ocean Research, Vol 102, 102299.

[18] Wanhai Xu, Qiannan Zhang, Wenchen Ma, Enhao Wang. (2020). “Response of two unequal diameter flexible cylinders in a side-by-side arrangement: characteristics of FIV,” China Ocean Engineering, Vol 34, pages 475-787.

[19] De, A. and T. DebRoy, A perspective on residual stresses in welding. Science and Technology of Welding and Joining, 2011. 16(3): p. 204-208.

[20] Ueda, Y., H. Murakawa, and N. Ma, Welding deformation and residual stress prevention. 2012: Elsevier.

[21] Knoedel, P., S. Gkatzogiannis, and T. Ummenhofer, Practical aspects of welding residual stress simulation. Journal of Constructional Steel Research, 2017. 132: p. 83-96.

[22] Nasir, N.S.M., et al., Review on welding residual stress. Stress, 2006. 2(5): p. 8-10.

[23] Smith, M., et al., Accurate prediction of residual stress in stainless steel welds. Computational Materials Science, 2012. 54: p. 312-328.



[24] Yun, H. B., Eslami, E., & Zhou, L. (2018). Noncontact stress measurement from bare UHPC surface using Raman piezospectroscopy. *Journal of Raman Spectroscopy*, 49(9), 1540-1551.

UHPC Using Raman Piezospectroscopy (No. 19-00976).

[26] Lawrence, F., J. Burk, and J. Yung, Influence of residual stress on the predicted fatigue life of weldments, in *Residual stress effects in fatigue*. 1982, ASTM International.

[27] Barsoum, Z. and I. Barsoum, Residual stress effects on fatigue life of welded structures using LEFM. *Engineering failure analysis*, 2009. 16(1): p. 449-467.

[28] Sasahara, H., The effect on fatigue life of residual stress and surface hardness resulting from different cutting conditions of 0.45% C steel. *International Journal of Machine Tools and Manufacture*, 2005. 45(2): p. 131-136.

[29] Kah, P., R. Suoranta, and J. Martikainen, Advanced gas metal arc welding processes. *The International Journal of Advanced Manufacturing Technology*, 2013. 67(1): p. 655-674.

[30] Huang, H., Huang, M., Zhang, W., & Yang, S. (2020). Experimental study of predamaged columns strengthened by HPFL and BSP under combined load cases. *Structure and infrastructure engineering*, 1-18. doi: 10.1080/15732479.2020.1801768

[31] Li, X., Yang, X., Yi, D., Liu, B., Zhu, J., Li, J., Wang, L. (2021). Effects of NbC content on microstructural evolution and mechanical properties of laser cladded Fe50Mn30Co10Cr10-xNbC composite coatings. *Intermetallics*, 138. doi: 10.1016/j.intermet.2021.107309

[32] Xu, X., Yang, Y., Chen, L., Chen, X., Wu, T., Li, Y., Li, B. (2021). Optomechanical Wagon-Wheel Effects for Bidirectional Sorting of Dielectric Nanoparticles. *Laser & photonics reviews*, 15(6), 2000546. doi: 10.1002/lpor.202000546

[33] Liu, J., MAO, S., Song, S., Huang, L., Belfiore, L. A., Tang, J. (2021). Towards applicable photoacoustic micro-fluidic pumps: Tunable excitation wavelength and improved stability by fabrication of Ag-Au alloying nanoparticles. *Journal of alloys and compounds*, 884. doi: 10.1016/j.jallcom.2021.161091

[34] Zhao, J., Gao, J., Li, W., Qian, Y., Shen, X., Wang, X., Jin, C. (2021). A combinatory ferroelectric compound bridging simple ABO₃ and A-site-ordered quadruple perovskite. *Nature communications*, 12(1), 747. doi: 10.1038/s41467-020-20833-6

[35] Li, Z., He, X., Zhang, C., Wang, X., Zhang, S., Jia, Y., Jin, C. (2022). Superconductivity above 200 K discovered in superhydrides of calcium. *Nature communications*, 13(1), 2863. doi: 10.1038/s41467-022-30454-w



[36] Kah, P., et al., Usability of arc types in industrial welding. *International Journal of Mechanical and Materials Engineering*, 2014. 9(1): p. 1-12.

[37] Nejad, R. M., & Liu, Z. (2020). Effect of periodic overloads and spectrum loading on

Journal Pre-proofs

Mechanics, 110, 102796.

[38] Barsoum, Z., Residual stress analysis and fatigue of multi-pass welded tubular structures. *Engineering failure analysis*, 2008. 15(7): p. 863-874.

[39] Alipooramirabad, H., et al., Quantification of residual stresses in multi-pass welds using neutron diffraction. *Journal of materials processing technology*, 2015. 226: p. 40-49.

[40] Ji, S., et al., Influence of a welding sequence on the welding residual stress of a thick plate. *Modelling and simulation in materials science and engineering*, 2005. 13(4): p. 553.

[41] Liu, Y., Y. Yang, and D. Wang, A study on the residual stress during selective laser melting (SLM) of metallic powder. *The International Journal of Advanced Manufacturing Technology*, 2016. 87(1): p. 647-656.

[42] Deng, D. and H. Murakawa, Prediction of welding residual stress in multi-pass butt-welded modified 9Cr–1Mo steel pipe considering phase transformation effects. *Computational Materials Science*, 2006. 37(3): p. 209-219.

[43] Bai, Y., Nardi, D. C., Zhou, X., Picón, R. A., & Flórez-López, J. (2021). A new comprehensive model of damage for flexural subassemblies prone to fatigue. *Computers & Structures*, 256, 106639. doi: 10.1016/j.compstruc.2021.106639

[44] Zhou, X., Bai, Y., Nardi, D. C., Wang, Y., Wang, Y., Liu, Z., Flórez-López, J. (2022). Damage Evolution Modeling for Steel Structures Subjected to Combined High Cycle Fatigue and High-Intensity Dynamic Loadings. *International Journal of Structural Stability and Dynamics*, 22(03n04), 2240012. doi: 10.1142/S0219455422400120

[45] Xiao, G., Chen, B., Li, S., & Zhuo, X. (2022). Fatigue life analysis of aero-engine blades for abrasive belt grinding considering residual stress. *Engineering failure analysis*, 131, 105846. doi: 10.1016/j.engfailanal.2021.105846

[46] Guo, J., Xiao, C., Gao, J., Li, G., Wu, H., Chen, L., Qian, L. (2021). Interplay between counter-surface chemistry and mechanical activation in mechanochemical removal of N-faced GaN surface in humid ambient. *Tribology international*, 159, 107004. doi: 10.1016/j.triboint.2021.107004

[47] Liang, L., Xu, M., Chen, Y., Zhang, T., Tong, W., Liu, H., Li, H. (2021). Effect of welding thermal treatment on the microstructure and mechanical properties of nickel-based superalloy



fabricated by selective laser melting. Materials science & engineering. A, Structural materials: properties, microstructure and processing, 819, 141507. doi: 10.1016/j.msea.2021.141507

[48] Wang, H., Xie, J., Chen, Y., Liu, W., & Zhong, W. (2022). Effect of CoCrFeNiMn high

Journal Pre-proofs

NiTi/304SS joint. Journal of materials research and technology, 18, 1028-1037. doi: 10.1016/j.jmrt.2022.03.022

Highlights

- This paper aims to evaluate the residual stress and fatigue life of T-type welded joints
- The fatigue tests were conducted under uniaxial loading
- The compressive residual stress increases with an increase in weld pass
- The triple-pass welded joint obtained enhanced fatigue strength with optimum compressive residual stress
- Multi-pass welding in different directions influences the change of residual stress and fatigue life

Declaration of interests

The authors declare that they have no known competing financial interests or personal relationships that could have appeared to influence the work reported in this paper.

The authors declare the following financial interests/personal relationships which may be considered as potential competing interests:

Journal Pre-proofs